Shape Programming for Narrow Ribbons of Nematic Elastomers

SHAPE PROGRAMMING FOR NARROW RIBBONS OF NEMATIC ELASTOMERS

VIRGINIA AGOSTINIANI, ANTONIO DESIMONE, AND KONSTANTINOS KOUMATOS

Abstract. Using the theory of Γ-convergence, we derive from three-dimensional elasticity new one-dimensional models for non-Euclidean elastic ribbons, i.e. ribbons exhibiting spontaneous curvature and twist. We apply the models to shape-selection problems for thin films of nematic elastomers with twist and splay-bend texture of the nematic director. For the former, we discuss the possibility of helicoid-like shapes as an alternative to spiral ribbons.

MSC (2010): 74B20, 76A15, 74K10, 74K20.

Keywords: nematic elastomers, dimension reduction, rod theory.

1. Introduction

Shape morphing systems are common in Biology. They are used to control locomotion in unicellular organisms [8, 9] and to produce controlled motions in plants [6, 13, 18, 21, 33]. Differential swelling and shrinkage processes, partially hindered by fibers, lead to dynamical conformation changes which are essential in the life of many botanical systems [30]. Inspired by Nature, many attempts have been reported in the recent literature to engineer artificial shape-morphing systems based on synthetic soft materials [22, 26, 31] and the interest in the general topic of "shape programming" is steadily growing.

A useful tool has emerged in the mathematical literature to describe the mechanics of shape programming, namely, *non-Euclidean* structures (non-Euclidean plates and rods). These are elastic structures described by functionals which are minimised by configurations exhibiting nonzero curvature. The relevant energy functionals are often postulated on the basis of physical intuition [24] but, in more recent attempts, they are derived from three-dimensional models [4, 25, 29] through rigorous dimension reduction based on the theory of Γ-convergence, following the approach pioneered in [1, 20].

Liquid crystal elastomers (LCEs) provide an interesting model system for the study of shape programming. They are polymeric materials that respond to external stimuli (temperature, light, electric fields) by changing shape [2, 3, 5, 14, 15, 35] and are typically manufactured as thin films [7, 10, 11, 12]. Suitable textures of the nematic director imprinted at fabrication lead to thin structures with tunable and controllable spontaneous curvature, see [4, 27, 28, 34]. In particular, for the *twist* geometry (nematic director always parallel to the mid-plane of the film and rotating by $\pi/2$ from the bottom to the top surface of the film), it has been observed both experimentally and computationally [28, 32] that, depending on the aspect ratio of the mid-plane, either spiral ribbons (this is the case of large width over length aspect ratio) or helicoid-like shapes (this is the case of small width over length aspect ratio) emerge spontaneously.

In this paper, we provide a rigorous mathematical description of thin structures made of nematic elastomers (both in the case of twist and of splay-bend geometry) where the minimisers of the deduced energy functionals reproduce the experimentally observed configurations. Our analysis stems from the combination of two

main results: first, we use the 3D-to-2D dimension reduction result in [4] for (non-Euclidean) thin films of nematic elastomers, and, secondly, we use a non-Euclidean version of the 2D-to-1D dimension reduction result of [19], where a corrected version of the well-known Sadowsky functional is derived for the mechanical description of inextensible elastic ribbons. The reader is also referred to [17, 23] and all other papers in the same special issue of the Journal of Elasticity for more material on the mechanics of elastic ribbons.

Our results show that the technique of rigorous dimensional reduction based on Γ-convergence, far from being just a mathematical exercise, can provide a tool to *derive*, rather than *postulate*, the functional form and the material parameters (elastic constants, spontaneous curvature and twist, etc.) for dimensionally reduced models of thin structures. For example, the possibility of assigning an energy to helicoid-like shapes - which in the 1D reduced model are represented by rods with straight mid-line, zero flexural strain around the width axis (in short, *flexure*) and non-zero torsional strain (in short, *torsion*), see the second picture in Figure 4 - rests precisely on the fact that, in the narrow ribbon limit, the isometry constraint on the mid-plane of the 2D theory is lost. This is the origin of the "correction" [19] to Sadowsky's functional (visible in the regime where flexure α is smaller than torsion β in formula (3.8)), a correction that can only be obtained with a variational notion of convergence of energy functionals (Γ-convergence). We concentrate our discussion on liquid crystal elastomers, but clearly our method is applicable to more general systems, whenever differential spontaneous distortions in the cross section induce spontaneous flexure and torsion of the mid-line of the rod (see e.g. [31]).

The starting point of the subsequent analysis is a family of non-Euclidean plate models defined on a narrow strip of width ε cut out from the plane $(\mathsf{e}_1, \mathsf{e}_2)$ at an angle θ with the horizontal axis (see energy (2.5) below). In Section 2 we set-up our 2D model and show that minor modifications of the results of [19] allow us to derive, in the limit as $\varepsilon \downarrow 0$, the 1D model defined in (2.12)–(2.13). Again in Section 2, we observe that examples of our starting 2D theory are given by twist and splay-bend nematic LCE sheets, as obtained from 3D nonlinear elasticity in [4]. The special role of the e_1 basis vector emerges from these concrete examples as the direction of the nematic director in the bottom face of the LCE sheet, see Figure 1. The limiting 1D theory, which is a non-Euclidean rod theory, is then explicitly computed for twist and splay-bend LCE ribbons in Sections 3 and 4, respectively. In particular, the explicit expression of the limiting energy densities of the rods, depending on the flexural strain around the width axis and the torsional strain, and their minimisers, are given in Proposition 3.2 and Lemma 3.3 (in the twist case) and in Proposition 4.1 and Lemma 4.2 (in the splay-bend case). These minimisers represent spontaneous flexure and torsion of LCE rods and their explicit formulas are provided in some special cases in Remarks 3.1 and 4.2. Starting from these computed values of spontaneous flexure and torsion, we reconstruct the non-trivial configurations assumed by these rods in the absence of external loadings, see Figures 3 and 4, which have been observed in experiments [27, 28, 34].

2. A non-Euclidean Sadowsky functional

Let ω be an open planar domain of $\mathbb{R}^2$. In the framework of a nonlinear plate theory [20], we consider the bending energy

$$\int_\omega \Big\{ c_1 |A_{\hat{v}}(\hat{z}) - \bar{A}|^2 + c_2 \operatorname{tr}^2(A_{\hat{v}}(\hat{z}) - \bar{A}) + \bar{e} \Big\} \mathrm{d}\hat{z} \tag{2.1}$$

associated with a developable surface $\hat{v}(\omega)$, $\hat{v}$ being a deformation from ω to $\mathbb{R}^3$. In the previous expression, $A_{\hat{v}}(\cdot) \in \mathbb{R}^{2\times 2}_{\mathrm{sym}}$ denotes the second fundamental form of

$\hat{v}(\omega)$, $c_1 > 0$ and $c_2 > 0$ are material constants, and $\bar{A} \in \mathbb{R}^{2\times 2}_{\rm sym}$ and $\bar{e}$ represent a characteristic target curvature tensor and a characteristic nonnegative energy constant, respectively. Although the constant $\bar{e}$ is inessential in the problem of finding minimal energy configurations, we prefer not to drop it in order to emphasize that, due to the kinematic incompatibility of the spontaneous strains in the 3D parent model, elastic energy due to residual stresses will always be present in our system. In other words, all the non-Euclidean plate and rod models in this paper describe systems which are never stress-free. Moreover, the notation $\mathrm{tr}^2 A$ stands for the square of the trace of A. We recall that $A_{\hat{v}}$ can be expressed as $(\nabla\hat{v})^{\mathrm{T}}\nabla\hat{v}$, where $\hat{\nu} = \partial_{z_1}\hat{v} \wedge \partial_{z_2}\hat{v}$. In [4], the two-dimensional energy (2.1) has been rigorously derived from a three-dimensional model for thin films of nematic elastomers with *splay-bend* and *twist* orientation of the nematic directors along the thickness and the following explicit formulas have been obtained for $\bar{A}$

$$\bar{A}_S \,=\, k\,\mathrm{diag}(-1,0), \qquad \bar{A}_T \,=\, k\,\mathrm{diag}(-1,1), \qquad k := \frac{6\,\eta_0}{\pi^2 h_0}, \tag{2.2}$$

and for $\bar{e}$

$$\bar{e}_S \,=\, \mu\,(1+\lambda)\left(\frac{\pi^4-12}{32}\right)\frac{\eta_0^2}{h_0^2} \qquad \bar{e}_T \,=\, \mu\left(\frac{\pi^4-4\pi^2-48}{8\pi^4}\right)\frac{\eta_0^2}{h_0^2}. \tag{2.3}$$

We recall that, in the splay-bend and in the twist geometry, the nematic director continuously rotates by $\pi/2$ from being parallel to e_1 at the bottom face to being parallel to e_3 and e_2, respectively, at the top face, see the first two pictures of Figure 1. Here and throughout the paper we use the indices "S" and "T" for the quantities related to the splay-bend and the twist case, respectively. In the previous formulas, η_0 is a positive dimensionless parameter quantifying the magnitude of the spontaneous strain variation along the (small) thickness h_0 of the film, μ is the elastic shear modulus, and $\lambda + 2\mu/3$ is the bulk modulus. We remark that nematic LCEs are anisotropic materials: both the energy well structure and the elastic moduli are, in principle, anisotropic. Since, however, experimental data on the elastic moduli are not currently available, most 3D models neglect the anisotropy of the elastic constants since many of the observed effects of anisotropy are already accounted for by the (anisotropic) structure of the energy wells (see e.g. [16]). This leads to anisotropic 2D energies such as (2.1), in which the anisotropy is confined to the target curvature, while the elastic constants only contain the Lamé coefficients typical of an isotropic material, see [4]. Also, the material constants appearing in (2.1) are given by

$$c_1 = \frac{\mu}{12}, \qquad c_2 = \frac{\lambda\mu}{12}. \tag{2.4}$$

We refer the reader to [4] for a detailed description of the three-dimensional model and of the splay-bend and twist nematic director fields. In Sections 3 and 4 we specialize our results to the case where the curvature tensor $\bar{A}$ is of the form (2.2), while in the rest of this section we focus on a general energy density of type (2.1).

Denoting by $\{\mathsf{e}_1, \mathsf{e}_2\}$ the canonical basis of $\mathbb{R}^2$, we cut out of the planar region ω a narrow strip

$$S^\theta_\varepsilon := \Big\{ z_1\mathsf{e}^\theta_1 + z_2\mathsf{e}^\theta_2 : z_1 \in (-\ell/2,\ell/2),\ z_2 \in (-\varepsilon/2,\varepsilon/2)\Big\} \subset \omega, \qquad 0 \le \theta < \pi,$$

with

$$\mathsf{e}^\theta_i := R_\theta \mathsf{e}_i, \quad i = 1,2, \qquad R_\theta = \begin{pmatrix} \cos\theta & -\sin\theta \\ \sin\theta & \cos\theta \end{pmatrix},$$

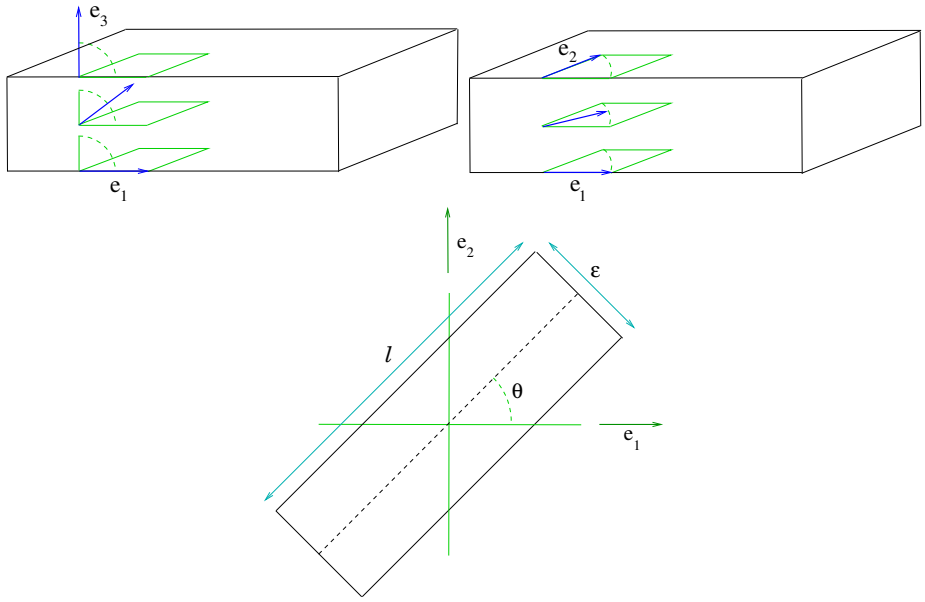

FIGURE 1. Top two pictures: distribution of the nematic directors along the thickness of the sheet, in the splay-bend and in the twist geometry, respectively. Bottom: a narrow strip S^θ_ε cut out of the mid-plane of the sheet, at an angle θ with the e_1-direction.

see the third picture of Figure 1, and consider the energy (2.1) restricted to the strip S^θ_ε, namely

$$\hat{\mathscr{E}}^\theta_\varepsilon(\hat{v}) := \int_{S^\theta_\varepsilon} \Big\{ c_1 |A_{\hat{v}}(\hat{z}) - \bar{A}\,|^2 + c_2 \operatorname{tr}^2(A_{\hat{v}}(\hat{z}) - \bar{A}\,) + \bar{e} \Big\}\, \mathrm{d}\hat{z}, \tag{2.5}$$

where $\hat{v} : S^\theta_\varepsilon \to \mathbb{R}^3$ is a deformation such that $\hat{v}(S^\theta_\varepsilon)$ is a developable surface. We are interested in examining the behaviour of the minimisers of the functionals $\hat{\mathscr{E}}^\theta_\varepsilon$ in the limit of vanishing width, i.e. $\varepsilon \downarrow 0$. Notice that using the function $v : S_\varepsilon \to \mathbb{R}^3$ defined in the unrotated strip $S_\varepsilon := S^0_\varepsilon$ as $v(z) = \hat{v}(R_\theta z)$, we have that $v(S_\varepsilon)$ is developable and $\hat{\mathscr{E}}^\theta_\varepsilon(\hat{v})$ can be rewritten as

$$\begin{aligned} \hat{\mathscr{E}}^\theta_\varepsilon(\hat{v}) &= \int_{S_\varepsilon} \Big\{ c_1 |A_{\hat{v}}(R_\theta z) - \bar{A}\,|^2 + c_2 \operatorname{tr}^2(A_{\hat{v}}(R_\theta z) - \bar{A}\,) + \bar{e} \Big\}\, \mathrm{d}z \\ &= \int_{S_\varepsilon} \Big\{ c_1 |A_v(z) - R_\theta^{\mathrm{T}} \bar{A} R_\theta|^2 + c_2 \operatorname{tr}^2(A_v(z) - \bar{A}\,) + \bar{e} \Big\} \mathrm{d}z, \end{aligned}$$

where in the second equality we have used the fact that $A_{\hat{v}}(R_\theta z) = R_\theta A_v(z) R_\theta^{\mathrm{T}}$. Now, introducing a suitable rescaling and setting

$$\mathscr{E}^\theta_\varepsilon(v) := \frac{1}{\varepsilon} \int_{S_\varepsilon} \Big\{ c_1 |\, A_v(z) - \bar{A}^\theta\,|^2 + c_2 \operatorname{tr}^2(A_v(z) - \bar{A}\,) + \bar{e} \Big\}\, \mathrm{d}z, \tag{2.6}$$

with

$$\bar{A}^\theta := R_\theta^{\mathrm{T}} \bar{A} R_\theta, \tag{2.7}$$

we have that $\hat{\mathscr{E}}^\theta_\varepsilon(\hat{v}) = \varepsilon\, \mathscr{E}^\theta_\varepsilon(v)$. Having this identification in mind, from now on we always deal with the functional $v \mapsto \mathscr{E}^\theta_\varepsilon(v)$. Expanding the integrand we obtain the following general form of the bending energy

$$\mathscr{E}^\theta_\varepsilon(v) = \frac{1}{\varepsilon} \int_{S_\varepsilon} \Big\{ c |A_v(z)|^2 + L^\theta(A_v(z)) \Big\}\, \mathrm{d}z, \tag{2.8}$$

where L^θ is the affine function defined as

$$L^\theta(A) := -2c_1 A\cdot \bar{A}^\theta - 2c_2 \operatorname{tr}A \operatorname{tr}\bar{A}^\theta + c_1|\bar{A}^\theta|^2 + c_2 \operatorname{tr}^2\bar{A}^\theta + \bar{e}. \tag{2.9}$$

In the above expression, we have set $c = c_1 + c_2$ and we have made use of the fact that

$$\operatorname{tr}^2 A = |A|^2 + 2\det A,$$

for all $A \in \mathbb{R}^{2\times 2}_{\rm sym}$. In fact, since v is an isometry of the planar strip S_ε, the Gaussian curvature associated with $v(S_\varepsilon)$ vanishes, i.e.

$$\det A_v(z) = 0.$$

The natural function space for v is the space of $\mathrm{W}^{2,2}$ isometries of S_ε defined as

$$\mathrm{W}^{2,2}_{\rm iso}(S_\varepsilon,\mathbb{R}^3) := \Big\{ v \in \mathrm{W}^{2,2}(S_\varepsilon,\mathbb{R}^3) \,:\, \partial_i v\cdot\partial_j v = \delta_{ij}\Big\}.$$

In order to express the energy over the fixed domain

$$S = I\times\Big(-\frac{1}{2},\frac{1}{2}\Big), \qquad\qquad I := \Big(-\frac{\ell}{2},\frac{\ell}{2}\Big),$$

we change variables and define the rescaled version $y : S \to \mathbb{R}^3$ of v, given by

$$y(x_1,x_2) = v(x_1,\varepsilon x_2).$$

The following procedure is rather standard and we use the notation of [19] as, in the sequel, our proofs will be largely based on this paper. By introducing the scaled gradient

$$\nabla_\varepsilon \cdot = (\partial_1 \cdot |\varepsilon^{-1}\partial_2 \cdot)$$

we obtain that $\nabla_\varepsilon y(x_1,x_2) = \nabla v(x_1,\varepsilon x_2)$ and y belongs to the space of scaled isometries of S defined as

$$\mathrm{W}^{2,2}_{{\rm iso},\varepsilon}(S,\mathbb{R}^3) := \Big\{ y \in \mathrm{W}^{2,2}(S,\mathbb{R}^3) \,:\, |\partial_1 y| = |\varepsilon^{-1}\partial_2 y| = 1,\ \partial_1 y\cdot\partial_2 y = 0 \text{ a.e. in } S\Big\}.$$

Similarly, we may define the scaled unit normal to $y(S)$ by

$$n_{y,\varepsilon} = \partial_1 y \wedge \varepsilon^{-1}\partial_2 y$$

and the scaled second fundamental form associated to $y(S)$ by

$$A_{y,\varepsilon} = \begin{pmatrix} n_{y,\varepsilon}\cdot\partial_1\partial_1 y & \varepsilon^{-1} n_{y,\varepsilon}\cdot\partial_1\partial_2 y \\ \varepsilon^{-1} n_{y,\varepsilon}\cdot\partial_1\partial_2 y & \varepsilon^{-2} n_{y,\varepsilon}\cdot\partial_2\partial_2 y \end{pmatrix}.$$

With this definition, $A_{y,\varepsilon}(x_1,x_2) = A_v(x_1,\varepsilon x_2)$ and $\mathscr{E}^\theta_\varepsilon(v) = \mathscr{J}^\theta_\varepsilon(y)$, where the functional

$$\mathscr{J}^\theta_\varepsilon(y) := \int_S \Big\{ c|A_{y,\varepsilon}|^2 + L^\theta(A_{y,\varepsilon})\Big\}\,\mathrm{d}x \tag{2.10}$$

is defined over the space $\mathrm{W}^{2,2}_{{\rm iso},\varepsilon}(S,\mathbb{R}^3)$ of scaled isometries of S.

Lemma 2.1 (Compactness)**.** *Suppose* $(y_\varepsilon)\subset \mathrm{W}^{2,2}_{{\rm iso},\varepsilon}(S,\mathbb{R}^3)$ *satisfy*

$$\sup_\varepsilon \mathscr{J}^\theta_\varepsilon(y_\varepsilon) < \infty.$$

Then, up to a subsequence and additive constants, there exist a deformation $y \in \mathrm{W}^{2,2}(I,\mathbb{R}^3)$ *and an orthonormal frame* $(d_1|d_2|d_3) \in \mathrm{W}^{1,2}(I,\mathrm{SO}(3))$ *fulfilling*

$$d_1 = y' \quad \text{ and } \quad d_1'\cdot d_2 = 0 \quad \text{ a.e. in } I,$$

and such that

$$y_\varepsilon \rightharpoonup y \quad \text{in} \quad \mathrm{W}^{2,2}(S,\mathbb{R}^3), \qquad\qquad \nabla_\varepsilon y_\varepsilon \rightharpoonup (d_1|d_2) \quad \text{in} \quad \mathrm{W}^{1,2}(S,\mathbb{R}^{3\times 2}).$$

Moreover, for some $\gamma \in \mathrm{L}^2(S,\mathbb{R}^3)$,

$$A_{y,\varepsilon} \rightharpoonup \begin{pmatrix} d_1'\cdot d_3 & d_2'\cdot d_3 \\ d_2'\cdot d_3 & \gamma \end{pmatrix} \quad \text{in} \quad \mathrm{L}^2(S,\mathbb{R}^{2\times 2}_{\rm sym}).$$

Proof. Note that

$$\begin{aligned}\mathscr{J}_\varepsilon^\theta(y_\varepsilon) &= \int_S \left\{ c_1 |A_{y_\varepsilon,\varepsilon} - \bar{A}^\theta|^2 + c_2 \operatorname{tr}^2\left(A_{y_\varepsilon,\varepsilon}(x) - \bar{A}^\theta\right) + \bar{e} \right\} \mathrm{d}x \\ &\geq \int_S c_1 |A_{y_\varepsilon,\varepsilon}(x) - \bar{A}^\theta|^2 \,\mathrm{d}x.\end{aligned}$$

But, since $\bar{A}^\theta$ is constant, this implies that $\|A_{y_\varepsilon,\varepsilon}\|^2_{\mathrm{L}^2(S,\mathbb{R}^3)}$ is bounded uniformly in ε and the proof is identical to the proof of Lemma 2.1 in [19]. □

In order to state the Γ-convergence result, we define

$$\mathcal{A} := \left\{ (d_1, d_2, d_3) \,:\, (d_1|d_2|d_3) \in \mathrm{W}^{1,2}(I, \mathrm{SO}(3)),\ d_1' \cdot d_2 = 0 \text{ a.e. in } I \right\} \tag{2.11}$$

and the functional $\mathscr{J}^\theta : \mathcal{A} \to \mathbb{R}$ by

$$\mathscr{J}^\theta(d_1, d_2, d_3) := \int_I \overline{Q}^\theta(d_1' \cdot d_3, d_2' \cdot d_3)\,\mathrm{d}x_1, \tag{2.12}$$

where

$$\overline{Q}^\theta(\alpha, \beta) := \min_{\gamma \in \mathbb{R}} \left\{ c|M|^2 + 2c|\det M| + L^\theta(M) \,:\, M = \begin{pmatrix} \alpha & \beta \\ \beta & \gamma \end{pmatrix} \right\}, \tag{2.13}$$

and $L^\theta(M)$ is defined according to (2.9). We recall that the constraint $d_1' \cdot d_2 = 0$ means that the narrow strip does not bend within its plane or, equivalently, that there is no flexure around the direction of d_3. Moreover, the quantities $d_1' \cdot d_3$ and $d_2' \cdot d_3$ have the physical meaning of flexural strain around d_2 and of torsional strain. To be short, throughout the paper we refer to them as *flexure* and *torsion*.

The proposition below provides an alternative expression for $\overline{Q}^\theta$ which is used heavily in the sequel. For the ease of the reader, we postpone its proof until the end of this section.

Proposition 2.2. *$\overline{Q}^\theta$ is a continuous function given by*

$$\overline{Q}^\theta(\alpha, \beta) = \begin{cases} -\frac{l_1^2}{4c} - l_1\alpha + l_2, & \text{in } \mathcal{D} \\ 4c\beta^2 - \frac{l_1^2}{4c} + l_1\alpha + l_2, & \text{in } \mathcal{U} \\ c\left(\frac{\alpha^2+\beta^2}{\alpha}\right)^2 + l_1\frac{\beta^2}{\alpha} + l_2, & \text{in } \mathcal{V}, \end{cases} \tag{2.14}$$

where $l_1 = l_1(\bar{A}^\theta)$, $l_2 = l_2(\alpha, \beta, \bar{A}^\theta)$ is an affine function of α and β, and

$$\mathcal{D} := \left\{ (\alpha, \beta) \in \mathbb{R}^2 : -\frac{l_1}{2c}\alpha > \beta^2 + \alpha^2 \right\}, \tag{2.15}$$

$$\mathcal{U} := \left\{ (\alpha, \beta) \in \mathbb{R}^2 : -\frac{l_1}{2c}\alpha \leq \beta^2 - \alpha^2 \right\}, \tag{2.16}$$

$$\mathcal{V} := \mathbb{R}^2 \setminus (\mathcal{D} \cup \mathcal{U}). \tag{2.17}$$

Theorem 2.3 (Γ-convergence)**.** *The functionals $\mathscr{J}_\varepsilon^\theta$ Γ-converge to $\mathscr{J}^\theta$ as $\varepsilon \to 0$ in the following sense:*

(1) *(Γ-lim inf inequality) for every sequence $(y_\varepsilon) \subset \mathrm{W}^{2,2}_{\mathrm{iso},\varepsilon}(S, \mathbb{R}^3)$, $y \in W^{2,2}(I, \mathbb{R}^3)$ and $(d_1, d_2, d_3) \in \mathcal{A}$ with $y' = d_1$ a.e. in I, $y_\varepsilon \rightharpoonup y$ in $\mathrm{W}^{2,2}(S, \mathbb{R}^3)$ and $\nabla_\varepsilon y_\varepsilon \rightharpoonup (d_1|d_2)$ in $\mathrm{W}^{1,2}(S, \mathbb{R}^{3\times 2})$, we have*

$$\liminf_{\varepsilon \to 0} \mathscr{J}_\varepsilon^\theta(y_\varepsilon) \geq \mathscr{J}^\theta(d_1, d_2, d_3);$$

(2) (*recovery sequence*) *for every* $(d_1, d_2, d_3) \in \mathcal{A}$ *there exists* $(y_\varepsilon) \subset \mathrm{W}^{2,2}_{\mathrm{iso},\varepsilon}(S, \mathbb{R}^3)$ *and (up to an additive constant)* y *satisfying* $y' = d_1$ *such that* $y_\varepsilon \rightharpoonup y$ *in* $\mathrm{W}^{2,2}(S, \mathbb{R}^3)$, $\nabla_\varepsilon y_\varepsilon \rightharpoonup (d_1|d_2)$ *in* $\mathrm{W}^{1,2}(S, \mathbb{R}^{3\times 2})$, *and*

$$\lim_{\varepsilon\to 0} \mathscr{J}^\theta_\varepsilon(y_\varepsilon) = \mathscr{J}^\theta(d_1, d_2, d_3).$$

In proving the existence of a recovery sequence, we will need the following lemma which is a slight variation of [19, Lemma 3.1].

Lemma 2.4. *For every* $M \in \mathrm{L}^2(I, \mathbb{R}^{2\times 2}_{\mathrm{sym}})$ *there exists a sequence* $(M_n) \subset \mathrm{L}^2(I, \mathbb{R}^{2\times 2}_{\mathrm{sym}})$ *satisfying* $\det M_n = 0$ *a.e. in* I *and for all* $n \in \mathbb{N}$ *such that* $M_n \rightharpoonup M$ *in* $\mathrm{L}^2(I, \mathbb{R}^{2\times 2}_{\mathrm{sym}})$ *and*

$$\int_I \left[c|M_n|^2 + L^\theta(M_n)\right] \mathrm{d}x_1 \longrightarrow \int_I \left[c|M|^2 + 2c|\det M| + L^\theta(M)\right] \mathrm{d}x_1.$$

Proof. The construction of the sequence M_n is identical to that in [19, Lemma 3.1]. To pass to the limit as $n \to \infty$, simply note that

$$\int_I L^\theta(M_n)\mathrm{d}x_1 \longrightarrow \int_I L^\theta(M)\mathrm{d}x_1,$$

since L^θ is affine. □

Proof of Theorem 2.3.
(1) (Γ-lim inf inequality) Let $(y_\varepsilon) \subset \mathrm{W}^{2,2}_{\mathrm{iso},\varepsilon}(S, \mathbb{R}^3)$, $y \in W^{2,2}(I, \mathbb{R}^3)$ and $(d_1, d_2, d_3) \in \mathcal{A}$ with $y' = d_1$ a.e. in I, $y_\varepsilon \rightharpoonup y$ in $\mathrm{W}^{2,2}(S, \mathbb{R}^3)$ and $\nabla_\varepsilon y_\varepsilon \rightharpoonup (d_1|d_2)$ in $\mathrm{W}^{1,2}(S, \mathbb{R}^3)$. We may assume that $\liminf_\varepsilon \mathscr{J}^\theta_\varepsilon(y_\varepsilon) < \infty$, as otherwise the result follows trivially, and by passing to a subsequence that $\sup_\varepsilon \mathscr{J}^\theta_\varepsilon(y_\varepsilon) < \infty$.

Lemma 2.1 now states that $A^\varepsilon := A_{y_\varepsilon,\varepsilon} \rightharpoonup A$ in $\mathrm{L}^2(S, \mathbb{R}^{2\times 2}_{\mathrm{sym}})$ where

$$A = \begin{pmatrix} d_1' \cdot d_3 & d_2' \cdot d_3 \\ d_2' \cdot d_3 & \gamma \end{pmatrix}.$$

We may now estimate

$$\begin{aligned}
\liminf_\varepsilon \mathscr{J}^\theta_\varepsilon(y_\varepsilon) &= \liminf_\varepsilon \int_S c|A^\varepsilon|^2 \,\mathrm{d}x + \lim_\varepsilon \int_S L^\theta(A^\varepsilon)\,\mathrm{d}x \\
&\geq \int_S \left[c|A|^2 + 2c|\det A|\right] + \int_S L^\theta(A)\,\mathrm{d}x \\
&\geq \mathscr{J}^\theta(d_1, d_2, d_3),
\end{aligned}$$

where the first integral is estimated exactly as in [19] and, since L^θ is affine, the second integral is weakly continuous.
(2) (recovery sequence) Fix $(d_1, d_2, d_3) \in \mathcal{A}$ and $y \in \mathrm{W}^{2,2}(I, \mathbb{R}^3)$ such that $y' = d_1$ a.e. in I. Define $R := (y'|d_2|d_3) \in \mathrm{SO}(3)$ a.e. in I and

$$M = \begin{pmatrix} y'' \cdot d_3 & d_2' \cdot d_3 \\ d_2' \cdot d_3 & \gamma \end{pmatrix},$$

where, for a.e. $x_1 \in I$, $\gamma(x_1)$ is chosen to be the value realising the minimum in (2.13) with $\alpha = y''(x_1) \cdot d_3(x_1)$, $\beta = d_2'(x_1) \cdot d_3(x_1)$. Namely,

$$\overline{Q}^\theta(y'' \cdot d_3, d_2' \cdot d_3) \;=\; c|M|^2 + 2c|\det M| + L^\theta(M) \qquad \text{a.e. in } I.$$

Note that, due to the precise form of γ given by (2.18) in the proof of Proposition 2.2 at the end of this section, we have that

$$\begin{aligned}
\gamma \;=\; (-l_1/2c - M_{11})\chi_{\left\{-\frac{l_1}{2c}M_{11} > M_{12}^2 + M_{11}^2\right\}} \;+\; (-l_1/2c + M_{11})\chi_{\left\{-\frac{l_1}{2c}M_{11} \leq M_{12}^2 - M_{11}^2\right\}} \\
+\; \frac{M_{12}^2}{M_{11}}\chi_{\left\{M_{12}^2 - M_{11}^2 < -\frac{l_1}{2c}M_{11} \leq M_{12}^2 + M_{11}^2\right\}}
\end{aligned}$$

where $M_{11} := y'' \cdot d_3$, $M_{12} := d_2' \cdot d_3$, and l_1 is a θ-dependent constant. From this fact, it is easy to deduce that $\gamma \in \mathrm{L}^2(I)$, considering that $M_{11} \in \mathrm{L}^2(I)$.

Through Lemma 2.4 we may then find a sequence $(M_n) \subset \mathrm{L}^2(I, \mathbb{R}^{2\times 2}_{\mathrm{sym}})$ such that $\det M_n = 0$, $M_n \rightharpoonup M$ in $\mathrm{L}^2(I, \mathbb{R}^{2\times 2}_{\mathrm{sym}})$ and, as $n \to \infty$,

$$\int_I \left[c|M_n|^2 + L^\theta(M_n)\right] \,\mathrm{d}x_1 \longrightarrow \int_I \left[c|M|^2 + 2c|\det M| + L^\theta(M)\right] \,\mathrm{d}x_1.$$

Performing the same construction as in [19], we find a sequence y^j_ε with the property that the associated second fundamental forms $A_{y^j_\varepsilon,\varepsilon}$ satisfy

$$A_{y^j_\varepsilon,\varepsilon} \to M^j \text{ strongly in } \mathrm{L}^2(S, \mathbb{R}^{2\times 2}_{\mathrm{sym}}) \text{ as } \varepsilon \to 0,$$

where the matrices M^j have been obtained by truncating and mollifying M_n and themselves satisfy $M^j \rightharpoonup M$ in $\mathrm{L}^2(I, \mathbb{R}^{2\times 2}_{\mathrm{sym}})$ as well as

$$\int_I c|M^j|^2 \,\mathrm{d}x_1 \longrightarrow \int_I \left[c|M|^2 + 2c|\det M|\right] \,\mathrm{d}x_1.$$

Then, since L^θ is affine, we deduce that

$$\begin{aligned}
\lim_{\varepsilon\to 0} \mathscr{J}^\theta_\varepsilon(y^j_\varepsilon) &= \lim_{\varepsilon\to 0} \int_S \left[c|A_{y^j_\varepsilon,\varepsilon}|^2 + L^\theta(A_{y^j_\varepsilon,\varepsilon})\right] \,\mathrm{d}x \\
&= \int_S \left[c|M^j|^2 + L^\theta(M^j)\right] \,\mathrm{d}x \\
&\overset{j\to\infty}{\longrightarrow} \int_S \left[c|M|^2 + 2c|\det M| + L^\theta(M)\right] \,\mathrm{d}x \\
&= \int_S \overline{Q}^{\,\theta}(d_1' \cdot d_3, d_2' \cdot d_3) \,\mathrm{d}x_1 = \mathscr{J}^\theta(d_1, d_2, d_3).
\end{aligned}$$

The proof can then be concluded by taking diagonal sequences. □

We end this section with the proof of Proposition 2.2.

Proof of Proposition 2.2. For a matrix

$$M = \begin{pmatrix} \alpha & \beta \\ \beta & \gamma \end{pmatrix},$$

the expression for $\overline{Q}^{\,\theta}$ in (2.13) becomes

$$\overline{Q}^{\,\theta}(\alpha, \beta) = \min_{\gamma\in\mathbb{R}} f(\gamma),$$

where

$$f(\gamma) := c(\alpha^2 + 2\beta^2 + \gamma^2) + 2c|\alpha\gamma - \beta^2| + l(\gamma).$$

Here, l is an affine function of γ

$$l(\gamma) = l_1\gamma + l_2,$$

with $l_1 = l_1(\bar{A}^\theta)$, and $l_2 = l_2(\alpha, \beta, \bar{A}^\theta)$ affine in α and β. Note that if $\alpha = 0$, f reduces to the differentiable function

$$f(\gamma) = 4c\beta^2 + c\gamma^2 + l(\gamma)$$

and it is minimised at $\gamma = -\frac{l_1}{2c}$, i.e. for all $\beta \in \mathbb{R}$

$$\overline{Q}^{\,\theta}(0, \beta) = 4c\beta^2 - \frac{l_1^2}{4c} + l_2.$$

Next assume that $\alpha \neq 0$. If $\gamma = \beta^2/\alpha$,

$$f(\beta^2/\alpha) = c\Big(\frac{\alpha^2 + \beta^2}{\alpha}\Big)^2 + l_1\frac{\beta^2}{\alpha} + l_2$$

and for any $\gamma \neq \beta^2/\alpha$, the function f is differentiable with

$$f'(\gamma) = 2c\gamma + 2c\alpha\,\mathrm{sgn}(\alpha\gamma - \beta^2) + l_1,$$

which vanishes if

$$\gamma = -\frac{l_1}{2c} - \alpha\,\mathrm{sgn}(\alpha\gamma - \beta^2).$$

If $\alpha\gamma > \beta^2$, then $\gamma_1 = -\frac{l_1}{2c} - \alpha$ is the critical point and this can only be true in the regime

$$-\frac{l_1}{2c}\alpha > \beta^2 + \alpha^2.$$

In this case, we compute

$$f(\gamma_1) = -\frac{l_1^2}{4c} - l_1\alpha + l_2.$$

Similarly, for $\alpha\gamma < \beta^2$, we find that $\gamma_2 = -\frac{l_1}{2c} + \alpha$ is the critical point which can only be true in the regime

$$-\frac{l_1}{2c}\alpha < \beta^2 - \alpha^2$$

and then

$$f(\gamma_2) = 4c\beta^2 - \frac{l_1^2}{4c} + l_1\alpha + l_2.$$

On the other hand, in the regime

$$\beta^2 - \alpha^2 \leq -\frac{l_1}{2c}\alpha \leq \beta^2 + \alpha^2,$$

a straightforward computation shows that $f'(\gamma) < 0$ if $\gamma < \beta^2/\alpha$ and $f'(\gamma) > 0$ if $\gamma > \beta^2/\alpha$. Hence, in this regime, and with $\alpha \neq 0$, the minimum value of f is achieved at $\gamma = \beta^2/\alpha$ so that

$$\overline{Q}^{\,\theta}(\alpha, \beta) = f(\beta^2/\alpha) = c\Big(\frac{\alpha^2 + \beta^2}{\alpha}\Big)^2 + l_1\frac{\beta^2}{\alpha} + l_2.$$

To compute $\overline{Q}^{\,\theta}$ in the respective regimes of values of $l_1\alpha$, one needs to understand whether the value of f at its respective local minima γ_1 and γ_2 is lower than $f(\beta^2/\alpha)$. We compute

$$\begin{aligned} f(\gamma_1) - f(\beta^2/\alpha) &= -c\left\{\frac{l_1^2}{4c^2} + \left(\frac{\alpha^2 + \beta^2}{\alpha}\right)^2 + l_1\frac{\alpha^2 + \beta^2}{\alpha}\right\} \\ &= -c\Big(\frac{\alpha^2 + \beta^2}{\alpha} + \frac{l_1}{2c}\Big)^2 \leq 0 \end{aligned}$$

with equality if and only if

$$-\frac{l_1}{2c}\alpha = \beta^2 + \alpha^2.$$

Similarly,

$$\begin{aligned} f(\gamma_2) - f(\beta^2/\alpha) &= -c\left\{\frac{l_1^2}{4c^2} + \left(\frac{\alpha^2 - \beta^2}{\alpha}\right)^2 - l_1\frac{\alpha^2 - \beta^2}{\alpha}\right\} \\ &= -c\Big(\frac{\alpha^2 - \beta^2}{\alpha} - \frac{l_1}{2c}\Big)^2 \leq 0 \end{aligned}$$

with equality if and only if

$$-\frac{l_1}{2c}\alpha = \beta^2 - \alpha^2.$$

Hence, we deduce the result. Note that these computations show that $\overline{Q}^{\,\theta}$ is continuous and that the value of $\gamma = \gamma(\alpha, \beta, \theta)$ realising the minimum in (2.13) is given by

$$\gamma(\alpha,\beta,\theta) \,=\, \begin{cases} -l_1/2c - \alpha, & \text{in } \ \mathcal{D} \\ -l_1/2c + \alpha, & \text{in } \ \mathcal{U} \\ \beta^2/\alpha, & \text{in } \ \mathcal{V}, \end{cases} \tag{2.18}$$

where the sets $\mathcal{U}$, $\mathcal{D}$, and $\mathcal{V}$ are defined in (2.16)–(2.17).

□

3. The twist case

In the case where the (physical) energy (2.5) is derived from a three-dimensional model with a twist-type nematic director field imprinted in the thickness of a LCE thin film, the characteristic quantities $\bar{A}$ and $\bar{e}$ present in (2.5) are given by $\bar{A}_T$ and $\bar{e}_T$ in formulas (2.2) and (2.3). Correspondingly, the θ-dependent target curvature tensor $\bar{A}^\theta$ defined in (2.7) becomes

$$\bar{A}^\theta_T \,=\, k \begin{pmatrix} -a_\theta & b_\theta \\ b_\theta & a_\theta \end{pmatrix}, \qquad a_\theta := \cos 2\theta, \quad b_\theta := \sin 2\theta, \quad \theta \in [0,\pi), \tag{3.1}$$

and $\mathrm{tr}\bar{A}^\theta_T = \mathrm{tr}\bar{A}_T = 0$. Moreover, the functional $\mathscr{E}^\theta_\varepsilon$ defined in (2.8) in this case reads

$$\mathscr{E}^\theta_{\varepsilon,T}(v) \,:=\, \frac{1}{\varepsilon}\int_{S_\varepsilon} \Big\{ c|A_v(z)|^2 + L^\theta_T(A_v(z)) \Big\} \mathrm{d}z,$$

with

$$L^\theta_T(A) \,:=\, -2c_1\, A\cdot \bar{A}^\theta_T + 2c_1 k^2 + \bar{e}_T.$$

Also, the energy $\mathscr{J}^\theta_\varepsilon$ defined in the rescaled configuration S (see (2.10)) is

$$\mathscr{J}^\theta_{\varepsilon,T}(y) := \int_S \Big\{ c|A_{y,\varepsilon}(x)|^2 + L^\theta_T(A_{y,\varepsilon}(x)) \Big\}\, \mathrm{d}x, \tag{3.2}$$

for every $y \in \mathrm{W}^{2,2}_{\mathrm{iso},\varepsilon}(S,\mathbb{R}^3)$. We recall that $\hat{\mathscr{E}}^\theta_\varepsilon(\hat{v}) = \varepsilon\, \mathscr{E}^\theta_\varepsilon(v) = \varepsilon\, \mathscr{J}^\theta_\varepsilon(y)$, where $\hat{v} : S^\theta_\varepsilon \to \mathbb{R}^3$, $v : S_\varepsilon \to \mathbb{R}^3$, $y : S \to \mathbb{R}^3$ are isometries and are related to each other via the following relations

$$v(z) = \hat{v}(R_\theta z), \qquad\qquad y(x_1,x_2) = v(x_1, \varepsilon x_2).$$

Lemma 2.1 and Theorem 2.3 apply in particular to the functionals (3.2), and the following corollary can be proved by standard arguments of the theory of Γ-convergence. In order to state it, we define $\mathscr{J}^\theta_T : \mathcal{A} \to \mathbb{R}$ as

$$\mathscr{J}^\theta_T(d_1,d_2,d_3) \,:=\, \int_I \overline{Q}^\theta_T(d_1'\cdot d_3, d_2'\cdot d_3)\, \mathrm{d}x_1, \tag{3.3}$$

where $\mathcal{A}$ is the class of orthonormal frames defined in (2.11) and $\overline{Q}^\theta_T$ is defined as in (2.13) with L^θ_T in place of L^θ (see also above).

Corollary 3.1. *If $(y_\varepsilon) \subset \mathrm{W}^{2,2}_{\mathrm{iso},\varepsilon}(S,\mathbb{R}^3)$ is a sequence of minimisers of $\mathscr{J}^\theta_{\varepsilon,T}$ then, up to a subsequence, there exist $y \in \mathrm{W}^{2,2}(I,\mathbb{R}^3)$ and a minimiser $(d_1|d_2|d_3) \in \mathcal{A}$ of $\mathscr{J}^\theta_T$ with $d_1 = y'$ such that*

$$y_\varepsilon \rightharpoonup y \ \ \text{in} \ \ \mathrm{W}^{2,2}(S,\mathbb{R}^3), \qquad \nabla_\varepsilon y_\varepsilon \rightharpoonup (d_1|d_2) \ \ \text{in} \ \ \mathrm{W}^{1,2}(S,\mathbb{R}^{3\times 2}),$$

and

$$A_{y,\varepsilon} \rightharpoonup \begin{pmatrix} d_1'\cdot d_3 & d_2'\cdot d_3 \\ d_2'\cdot d_3 & \gamma \end{pmatrix} \ \ \text{in} \ \ \mathrm{L}^2(S,\mathbb{R}^{2\times 2}_{\mathrm{sym}}), \qquad \text{for some} \ \ \gamma \in \mathrm{L}^2(S,\mathbb{R}^3). \tag{3.4}$$

Moreover,

$$\min_{\mathrm{W}^{2,2}_{\mathrm{iso},\varepsilon}(S,\mathbb{R}^3)} \mathscr{J}^\theta_{\varepsilon,T} \longrightarrow \min_{\mathcal{A}} \mathscr{J}^\theta_T.$$

The following proposition gives the explicit expression of $\overline{Q}_T^{\,\theta}$.

Proposition 3.2. *$\overline{Q}_T^{\,\theta}$ is a continuous function given by*

$$\overline{Q}_T^{\,\theta}(\alpha,\beta) \;=\; \begin{cases} 4c_1k\big(a_\theta\alpha - b_\theta\beta\big) + c_1k^2\Big(2 - \frac{c_1}{c}a_\theta^2\Big) + \bar{e}_T, & \text{in} \quad \mathcal{D}_T \\ 4\big(c\beta^2 - c_1kb_\theta\beta\big) + c_1k^2\Big(2 - \frac{c_1}{c}a_\theta^2\Big) + \bar{e}_T, & \text{in} \quad \mathcal{U}_T \\ c\frac{(\alpha^2+\beta^2)^2}{\alpha^2} + 2c_1k\Big(a_\theta\frac{\alpha^2-\beta^2}{\alpha} - 2b_\theta\beta\Big) + 2c_1k^2 + \bar{e}_T, & \text{in} \quad \mathcal{V}_T, \end{cases}$$

where a_θ and b_θ are defined in (3.1)*, and*

$$\mathcal{D}_T := \Big\{(\alpha,\beta)\in\mathbb{R}^2 : \frac{c_1}{c}ka_\theta\,\alpha > \beta^2+\alpha^2\Big\}, \tag{3.5}$$

$$\mathcal{U}_T := \Big\{(\alpha,\beta)\in\mathbb{R}^2 : \frac{c_1}{c}ka_\theta\,\alpha \le \beta^2-\alpha^2\Big\}, \tag{3.6}$$

$$\mathcal{V}_T := \mathbb{R}^2 \setminus (\mathcal{D}_T \cup \mathcal{U}_T). \tag{3.7}$$

Proof. It suffices to calculate the coefficients $l_1(\bar{A}_T^\theta)$ and $l_2(\alpha,\beta,\bar{A}_T^\theta)$ for the case of the twist geometry. An easy computation shows that

$$l_1(\bar{A}_T^\theta) = -2c_1ka_\theta$$

and

$$l_2(\alpha,\beta,\bar{A}_T^\theta) = 2c_1ka_\theta\alpha - 4c_1kb_\theta\beta + 2c_1k^2 + \bar{e}_T.$$

The result now follows by Proposition 2.2. □

Note that when $k=0$ (and $c=1$), modulo the constant $\bar{e}_T$, the expression for $\overline{Q}_T^{\,\theta}$ in Proposition 3.2 reduces to expression (1.5) in [19], namely,

$$\overline{Q}(\alpha,\beta) := \begin{cases} 4\,\beta^2 & \text{if} \quad \alpha^2 \le \beta^2 \\ \frac{(\alpha^2+\beta^2)^2}{\alpha^2} & \text{if} \quad \alpha^2 > \beta^2. \end{cases} \tag{3.8}$$

Indeed, in this case

$$\mathcal{D}_T = \emptyset, \qquad \mathcal{U}_T = \big\{(\alpha,\beta)\in\mathbb{R}^2 : \alpha^2 \le \beta^2\big\}. \tag{3.9}$$

For $k>0$, it is natural to distinguish the case $\theta=\pi/4$ (and, similarly, the case $\theta=3\pi/4$) from all the other cases. Indeed, we have $a_{\pi/4}=0$ and $b_{\pi/4}=1$, so that $\mathcal{D}_T$ and $\mathcal{U}_T$ are again given by (3.9), and

$$\overline{Q}_T^{\,\pi/4}(\alpha,\beta) = \begin{cases} 4\big(c\beta^2 - c_1k\beta\big) + 2c_1k^2 + \bar{e}_T, & \text{if} \quad \alpha^2 \le \beta^2 \\ c\frac{(\alpha^2+\beta^2)^2}{\alpha^2} - 4c_1k\beta + 2c_1k^2 + \bar{e}_T, & \text{if} \quad \alpha^2 > \beta^2. \end{cases}$$

We refer the reader to the last picture of Figure 2 (counting clockwise from the top left). Observe that for all $\theta\in[0,\pi/2)\setminus\{\pi/4,3\pi/4\}$, setting $\rho := c_1ka_\theta/(2c)$, we have that $\mathcal{D}_T$ coincides with the (open) disk $(\alpha-\rho)^2+\beta^2<\rho^2$ and $\mathcal{U}_T$ with the (closed) region inside the hyperbola $(\alpha+\rho)^2-\beta^2=\rho^2$, see the other three pictures of Figure 2.

We want to examine the minimisers of $\overline{Q}_T^{\,\theta}$. Observe that in the case $k=0$ the above function $(\alpha,\beta)\mapsto\overline{Q}(\alpha,\beta)$ is minimised by $(0,0)$. This means that the 1D energy (3.3) is minimised by a trivial configuration with zero flexure and torsion, i.e. in the absence of applied loads, the rod exhibits no spontaneous flexure or torsion. When instead $k>0$, we have that the minimisers of $\overline{Q}_T^{\,\theta}$ are non-trivial (in fact, they lie on a segment) and spontaneous flexure and torsion of the rod become possible. This is the content of the following lemma.

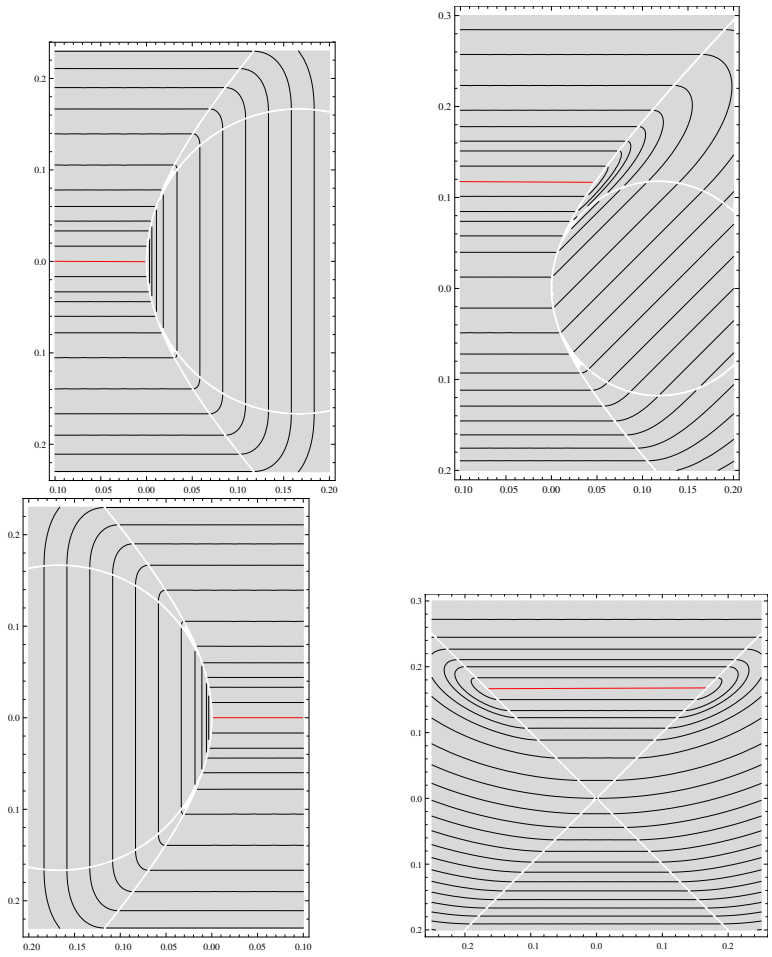

FIGURE 2. Phase diagrams in the (α, β)-plane, with level curves of $\overline{Q}^{\theta}_{T}$. The white lines emphasize the boundary of $\mathcal{V}_T$ (cf. (3.5)–(3.7)) and the red lines the set of minimisers. The pictures correspond to the cases $\theta = 0$, $\theta = \pi/8$, $\theta = \pi/4$, and $\theta = \pi/2$, respectively, counting clockwise from top left.

Lemma 3.3. *For every $0 \le \theta < \pi$, $\overline{Q}^{\theta}_{T}$ attains its minimum value precisely on the segment $\left[\alpha^T_{\theta,1}, \alpha^T_{\theta,2}\right] \times \{\beta_\theta\}$, where*

$$\beta_\theta := \frac{k\, c_1}{2\, c} \sin 2\theta,$$

and

$$\alpha^T_{\theta,1} := -\frac{k\, c_1}{2\, c}(1 + \cos 2\theta), \qquad \alpha^T_{\theta,2} := \frac{k\, c_1}{2\, c}(1 - \cos 2\theta).$$

Moreover,

$$\min_{\mathbb{R}^2} \overline{Q}^{\theta}_{T} \;=\; c_1 k^2 \left(2 - \frac{c_1}{c}\right) + \bar{e}_T. \tag{3.10}$$

Note that the segment $\left[\alpha^T_{\theta,1}, \alpha^T_{\theta,2}\right] \times \{\beta_\theta\}$ is a subset of $\mathcal{U}_T$ connecting the two branches of the hyperbola $\frac{c_1}{c} k a_\theta\, \alpha \le \beta^2 - \alpha^2$ (a degenerate hyperbola in the case $k = 0$ or $\theta \in \{\pi/4, 3\pi/4\}$).

Proof. Consider the nontrivial case $k \neq 0$. A straightforward computation shows that the points $(\alpha,\beta) \in \big(\alpha^T_{\theta,1}, \alpha^T_{\theta,2}\big) \times \{\beta_\theta\}$, which lie in the interior of $\mathcal{U}_T$, are local minimisers, and that $\overline{Q}^{\,\theta}_T$ evaluated at each of these points gives the value (3.10). At the same time, when $\mathcal{D}_T \neq \emptyset$, we have that $\nabla \overline{Q}_\theta(\alpha,\beta) \neq 0$ for every $(\alpha,\beta) \in \mathcal{D}_T$, because a_θ and b_θ can never vanish simultaneously. Moreover, a point (α,β) lying in the interior of $\mathcal{V}_T$ is a critical point of $\overline{Q}^{\,\theta}_T$ iff

$$c\,\alpha - c\,\frac{\beta^4}{\alpha^3} + c_1 k\, a_\theta \frac{\beta^2}{\alpha^2} + c_1 k\, a_\theta \;=\; 0, \tag{3.11}$$

$$c\,\frac{\beta^3}{\alpha^2} + c\,\beta - c_1 k\, a_\theta \frac{\beta}{\alpha} - c_1 k\, b_\theta \;=\; 0. \tag{3.12}$$

Now, observe that in the case $\beta \neq 0$, multiplying the second equation by β/α and adding the first yields

$$c\,(\alpha^2+\beta^2) + c_1 k\big(a_\theta \alpha + b_\theta \beta\big) \;=\; 0.$$

At the same time, equation (3.11) is equivalent to

$$c\,(\beta^2-\alpha^2) - c_1 k\, a_\theta \alpha \;=\; 0.$$

Summing up the last two equations gives $\beta = c_1 k b_\theta/(2c)$ and in turn $\alpha = \alpha^T_{\theta,1}$ or $\alpha = \alpha^T_{\theta,2}$, when $b_\theta \neq 0$. In the case $b_\theta = 0$, a similar argument gives that $(-c_1 k/c, 0)$ is the solution to (3.11)–(3.12). In any case, we have obtained that the solutions of (3.11)–(3.12) lie in $\partial\mathcal{U}_T$. Hence, there are no critical points of $\overline{Q}^{\,\theta}_T$ in the interior of $\mathcal{U}_T$. Other straightforward computations show that the values of $\overline{Q}^{\,\theta}_T$ on $\partial U_T \setminus \{(\alpha^T_{\theta,1},\beta_\theta), (\alpha^T_{\theta,2},\beta_\theta)\}$ are strictly smaller than the local minimum, therefore the local minimisers are indeed global. This concludes the proof of the lemma. □

Remark 3.1 (Spontaneously curved LCE twist ribbons). Using the above lemma we can now find the minimisers and the minimum of our limiting functional (3.3). Indeed, minimising the integrand pointwise, we have that

$$\begin{aligned}\min_{\mathcal{A}} \mathscr{J}^{\,\theta}_T \;=\; \ell \min_{\mathbb{R}^{2\times 2}} \overline{Q}^{\,\theta}_T \;&=\; \ell\left[c_1 k^2\left(2 - \frac{c_1}{c}\right) + \bar{e}_T\right] \\ &=\; \frac{\mu\,\ell}{\pi^4}\left[3\left(\frac{1+2\lambda}{1+\lambda}\right) + \frac{\pi^4 - 4\pi^2 - 48}{8}\right]\frac{\eta_0^2}{h_0^2},\end{aligned}$$

where in the second equality we have used (3.10) and in the last one the constants c_1, c, k, and $\bar{e}_T$ have been substituted with their expressions given in terms of the parameters of the 3D model (cf. (2.2)–(2.4)), which are amenable to direct measurement in the laboratory synthesizing the LCE specimen. The set $(\alpha,\beta) \in \big[\alpha^T_{\theta,1}, \alpha^T_{\theta,2}\big] \times \{\beta_\theta\}$ of the minimisers of $\overline{Q}^{\,\theta}_T$ is given by

$$\left[\frac{3\,\eta_0}{\pi^2(1+\lambda)\,h_0}(-a_\theta - 1)\,,\; \frac{3\,\eta_0}{\pi^2(1+\lambda)\,h_0}(1-a_\theta)\right] \times \left\{\frac{3\,\eta_0}{\pi^2(1+\lambda)\,h_0} b_\theta\right\}. \tag{3.13}$$

Hence, any $(d_1,d_2,d_3) \in \mathcal{A}$ such that the flexure $d_1' \cdot d_3$ and the torsion $d_2' \cdot d_3$ are constant and satisfy

$$d_1'\cdot d_3 \in \left[\frac{3\,\eta_0}{\pi^2(1+\lambda)\,h_0}(-a_\theta - 1)\,,\; \frac{3\,\eta_0}{\pi^2(1+\lambda)\,h_0}(1-a_\theta)\right], \quad d_2'\cdot d_3 \;=\; \frac{3\,\eta_0}{\pi^2(1+\lambda)\,h_0} b_\theta,$$

is a minimiser of $\mathscr{J}^{\,\theta}_T$. Indeed, given two continuous functions $I \ni x_1 \mapsto \alpha(x_1)$ and $I \ni x_1 \mapsto \beta(x_1)$, there always exists a $\mathrm{C}^1(I)$-solution to the problem

$$(d_1,d_2,d_3) \in \mathcal{A}, \qquad d_1' \cdot d_3 = \alpha, \qquad d_2' \cdot d_3 = \beta. \tag{3.14}$$

In particular, when α and β are constant, identifying (d_1, d_2, d_3) with the rotation matrix $Q = (d_1|d_2|d_3)$, it is standard to see that finding a solution of (3.14) consists in solving

$$Q'(s) = Q(s) \begin{pmatrix} 0 & 0 & -\alpha \\ 0 & 0 & -\beta \\ \alpha & \beta & 0 \end{pmatrix}, \tag{3.15}$$

for some fixed $Q(0) \in \mathrm{SO}(3)$, and that the solution $Q(s)$ is actually a rotation matrix. Also, once $s \mapsto d_1(s)$ is given, the mid-line curve is given by

$$r(s) = r(0) + \int_0^s d_1(\sigma) d\sigma \tag{3.16}$$

and it is fixed up to a translation. The last two equations allow us to reconstruct the rod configuration through its mid-line curve (3.16) and the orientation of the directors given by the solution to (3.15).

For the convenience of the reader, we consider explicitly two cases:

$$\theta = 0: \qquad (d_1' \cdot d_3, d_2' \cdot d_3) \in \left[-\frac{6\,\eta_0}{\pi^2(1+\lambda)\,h_0}\,, 0 \right] \times \{0\}\,,$$

$$\theta = \pi/4: \quad (d_1' \cdot d_3, d_2' \cdot d_3) \in \left[-\frac{3\,\eta_0}{\pi^2(1+\lambda)\,h_0}\,, \frac{3\,\eta_0}{\pi^2(1+\lambda)\,h_0} \right] \times \left\{ \frac{3\,\eta_0}{\pi^2(1+\lambda)\,h_0} \right\}.$$

Some examples of the corresponding rod configurations are shown in Figures 3 and 4, respectively. The configurations are rendered by plotting the mid-line curve $r(s)$ thickened along the direction $d_2(s)$ by a fixed, small amount.

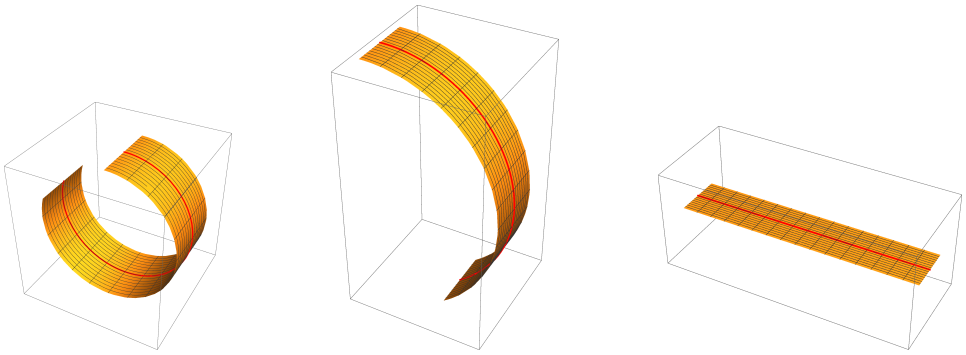

FIGURE 3. Some examples of minimal energy configurations for the 1D model (3.3) (where the energy density is given by Proposition 3.2), for the case $\theta = 0$. From left to right, the configurations are characterized by an increasing (constant) value of $\alpha = d_1' \cdot d_3$ in the admissible interval $\left[-\frac{6\,\eta_0}{\pi^2(1+\lambda)\,h_0}\,, 0 \right]$. In particular, in the last picture $\alpha = 0$. We plot the mid-line of the curve $s \mapsto r(s)$ (red line), and, at each point $r(s)$, a segment along the director $d_2(s)$ (yellow).

We note that the minimisers predicted by our limiting model are in agreement with [31, Figure 3], where minimum-energy configurations of self-shaping synthetic systems made of swelling hydrogels with oriented reinforcements are shown.

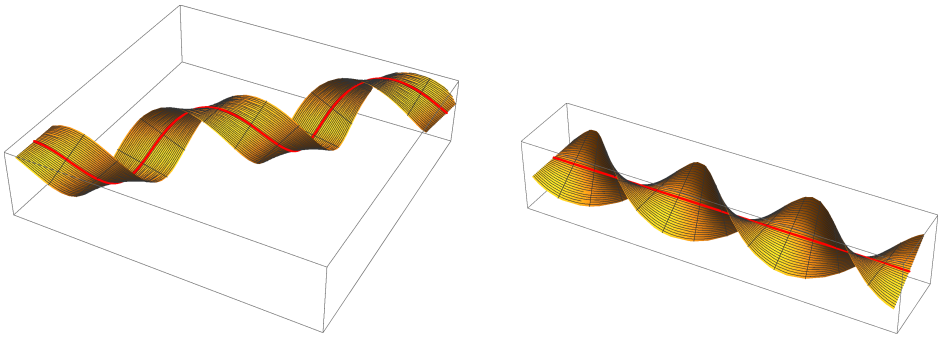

FIGURE 4. Two examples of minimal energy configurations for the 1D model (3.3), where the energy density is given by Proposition 3.2, for $\theta = \pi/4$. They are characterized by the same constant value $\beta = d_2' \cdot d_3$, and by two constant values of $\alpha = d_1' \cdot d_3$, taken in the admissible interval $\left[-\frac{3\,\eta_0}{\pi^2(1+\lambda)\,h_0}\,,\,\frac{3\,\eta_0}{\pi^2(1+\lambda)\,h_0}\right]$. In particular, the second configuration corresponds to $\alpha = 0$ and its mid-line is a straight line. In the other configuration the mid-line is a helix. We plot the mid-line of the curve $s \mapsto r(s)$ (red line), and, at each point $r(s)$, a segment along the director $d_2(s)$ (yellow).

4. The splay-bend case

In the splay-bend case, the θ-dependent target curvature tensor $\bar{A}^\theta$ defined in (2.7) is

$$\bar{A}^\theta_S = k \begin{pmatrix} -\cos^2\theta & \sin\theta\cos\theta \\ \sin\theta\cos\theta & -\sin^2\theta \end{pmatrix}$$

and $\det \bar{A}^\theta_S = \det \bar{A}_S = 0$. The functional defined in (2.8) becomes

$$\mathscr{E}^\theta_{\varepsilon,S}(v) = \frac{1}{\varepsilon}\int_{S_\varepsilon} \Big\{ c|A_v(z)|^2 + L^\theta_S(A_v(z)) \Big\} \mathrm{d}z,$$

with

$$L^\theta_S(A) \;:=\; -2c_1 A \cdot \bar{A}^\theta_S + 2c_2 k\,\mathrm{tr}A + ck^2 + \bar{e}_S.$$

Also, the rescaled energy (2.10) is now given by

$$\mathscr{J}^\theta_{\varepsilon,S}(y) := \int_S \Big\{ c|A_{y,\varepsilon}(x)|^2 + L^\theta_S(A_{y,\varepsilon}(x)) \Big\}\,\mathrm{d}x,$$

for every $y \in \mathrm{W}^{2,2}_{\mathrm{iso},\varepsilon}(S,\mathbb{R}^3)$, and $\mathscr{J}^\theta_S : \mathcal{A} \to \mathbb{R}$ is defined as

$$\mathscr{J}^\theta_S(d_1,d_2,d_3) \;:=\; \int_I \overline{Q}^\theta_S(d_1'\cdot d_3, d_2'\cdot d_3)\,\mathrm{d}x_1, \tag{4.1}$$

where $\overline{Q}^\theta_S$ is given by (2.13), with L^θ_S in place of L^θ. The counterpart of Corollary 3.1 holds for the splay-bend case: it is sufficient to replace $\mathscr{J}^\theta_{\varepsilon,T}$ and $\mathscr{J}^\theta_T$ by $\mathscr{J}^\theta_{\varepsilon,S}$ and $\mathscr{J}^\theta_S$, respectively, in the statement of Corollary 3.1.

Note that thanks to Lemma 4.2 below, the minimum of $\mathscr{J}^\theta_{\varepsilon,S}$ in $\mathrm{W}^{2,2}_{\mathrm{iso},\varepsilon}(S,\mathbb{R}^3)$ and the minimum of $\mathscr{J}^\theta_S$ in $\mathcal{A}$ can be computed explicitly, so that the convergence of the former to the latter can be checked by hand. The 2D minimizing rescaled second fundamental forms can be computed as well, together with the 1D minimal flexure and torsion, and with γ (cf. (3.4)). Therefore, also the convergence of the rescaled second fundamental forms can be checked by hand.

To proceed with our analysis, we note that $\bar{A}^\theta_S$ can be alternatively written as

$$\bar{A}^\theta_S = \frac{1}{2}\left(\bar{A}^\theta_T - \mathbb{I}\right)$$

and in turn

$$L^\theta_S(A) = -c_1 A \cdot \bar{A}^\theta_T + k(c+c_2)\,\mathrm{tr}A + ck^2 + \bar{e}_S.$$

Hence, setting $d_\theta = c_1 a_\theta - c - c_2$, we have that

$$\overline{Q}^\theta_S(\alpha,\beta) = \min_{\gamma\in\mathbb{R}} f(\gamma),$$

where

$$f(\gamma) := c(\alpha^2 + 2\beta^2 + \gamma^2) + 2c|\alpha\gamma - \beta^2| - kd_\theta(\alpha+\gamma) + 2kc_1(a_\theta\alpha - b_\theta\beta) + ck^2 + \bar{e}_S, \tag{4.2}$$

recalling that $a_\theta := \cos 2\theta$ and $b_\theta := \sin 2\theta$.

Proposition 4.1. *$\overline{Q}^\theta_S$ is a continuous function given by*

$$\overline{Q}^\theta_S(\alpha,\beta) = \begin{cases} 2c_1k\big(a_\theta\alpha - b_\theta\beta\big) + ck^2\Big(1 - \frac{d_\theta^2}{4c^2}\Big) + \bar{e}_S, & \text{in } \mathcal{D}_S \\ 4c\beta^2 - 2kd_\theta\alpha + 2c_1k\big(a_\theta\alpha - b_\theta\beta\big) + ck^2\Big(1 - \frac{d_\theta^2}{4c^2}\Big) + \bar{e}_S, & \text{in } \mathcal{U}_S \\ c\frac{(\alpha^2+\beta^2)^2}{\alpha^2} - kd_\theta\frac{\alpha^2+\beta^2}{\alpha} + 2c_1k\big(a_\theta\alpha - b_\theta\beta\big) + ck^2 + \bar{e}_S, & \text{in } \mathcal{V}_S, \end{cases}$$

where $d_\theta := c_1 a_\theta - c - c_2$, and

$$\mathcal{D}_S := \left\{(\alpha,\beta)\in\mathbb{R}^2 : \frac{k}{2c}d_\theta\,\alpha > \beta^2 + \alpha^2\right\}, \tag{4.3}$$

$$\mathcal{U}_S := \left\{(\alpha,\beta)\in\mathbb{R}^2 : \frac{k}{2c}d_\theta\,\alpha \le \beta^2 - \alpha^2\right\}, \tag{4.4}$$

$$\mathcal{V}_S := \mathbb{R}^2 \setminus (\mathcal{D}_S \cup \mathcal{U}_S). \tag{4.5}$$

Proof. By (4.2), we immediately deduce that

$$l_1(\bar{A}^\theta_S) = -kd_\theta$$

and

$$l_2(\alpha,\beta,\bar{A}^\theta_S) = -kd_\theta\alpha + 2kc_1(a_\theta\alpha - b_\theta\beta) + ck^2 + \bar{e}_S.$$

The result now follows by substituting these values in Proposition 2.2. □

We refer the reader to Figure 5 where plots of the level curves of $\overline{Q}^\theta_S$ are displayed for a selection of angles θ.

Remark 4.1. Setting

$$\overline{Q}^\theta_{S,1} := 2c_1k\big(a_\theta\alpha - b_\theta\beta\big) + ck^2\Big(1 - \frac{d_\theta^2}{4c^2}\Big) + \bar{e}_S,$$

we have that $\overline{Q}^\theta_S = \overline{Q}^\theta_{S,1}$ in $\mathcal{D}_S$, that

$$\overline{Q}^\theta_S = \overline{Q}^\theta_{S,2}(\alpha,\beta) := 4c\beta^2 - 2kd_\theta\alpha + \overline{Q}^\theta_{S,1}(\alpha,\beta) \qquad \text{in} \quad \mathcal{U}_S,$$

and that

$$\overline{Q}^\theta_S = c\Big(\frac{\alpha^2+\beta^2}{\alpha} - \frac{kd_\theta}{2c}\Big)^2 + \overline{Q}^\theta_{S,1}(\alpha,\beta) = c\Big(\frac{\beta^2-\alpha^2}{\alpha} - \frac{kd_\theta}{2c}\Big)^2 + \overline{Q}^\theta_{S,2}(\alpha,\beta) \quad \text{in} \quad \mathcal{V}_S.$$

Since the squares in these expressions vanish on $\partial\mathcal{D}_S$ and $\partial\mathcal{U}_S$, respectively, this shows in particular that $\overline{Q}^\theta_S$ is continuous.

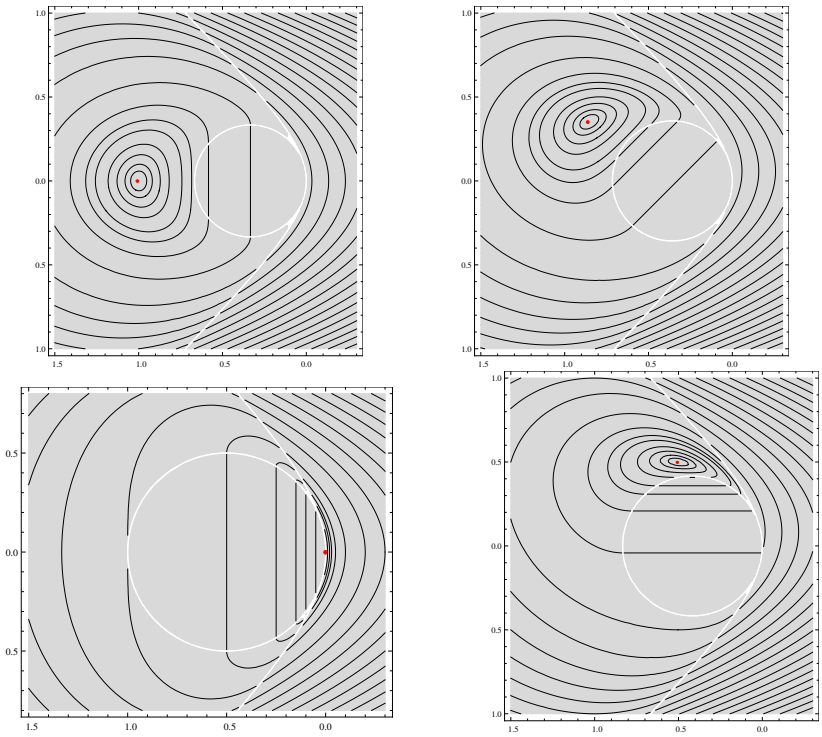

FIGURE 5. Phase diagrams in the (α, β)-plane, with level curves of $\overline{Q}_S^{\,\theta}$. The white lines emphasize the boundary of $\mathcal{V}_T$ (cf. (4.3)–(4.5)) and the red lines the set of minimisers. The pictures correspond to the cases $\theta = 0$, $\theta = \pi/8$, $\theta = \pi/4$, and $\theta = \pi/2$, respectively, counting clockwise from top left.

We now focus on the minimisers of $\overline{Q}_S^{\,\theta}$. As for the twist case, when $k = 0$ and up to additive and multiplicative constants, the function $\overline{Q}_S^{\,\theta}$ reduces to the function defined in (3.8), which is minimised at $(0, 0)$. When instead $k > 0$, differently from the twist case, we have that for every θ the minimiser of $\overline{Q}_S^{\,\theta}$ is a (θ-dependent) single point, in view of the following lemma.

Lemma 4.2. *For every $0 \le \theta < \pi$, $\overline{Q}_S^{\,\theta}$ is minimised precisely at $(\alpha_\theta^S, \beta_\theta^S)$, where*

$$\alpha_\theta^S := -\frac{k}{2}\big(1 + \cos 2\theta\big), \qquad \beta_\theta^S := \frac{k}{2}\sin 2\theta.$$

Moreover,

$$\min_{\mathbb{R}^2} \overline{Q}_S^{\,\theta} = \bar{e}_S. \tag{4.6}$$

Proof. Consider the nontrivial case $k \neq 0$. A straightforward computation shows that there are no critical points of $\overline{Q}_S^{\,\theta}$ in the interior of $\mathcal{D}_S$ or $\mathcal{U}_S$, for any value of θ. Next, we look for critical points in the interior of $\mathcal{V}_S$. Differentiating the first of

the two expressions for $\overline{Q}_S^\theta$ in $\mathcal{V}_S$ given in Remark 4.1 and setting $\nabla \overline{Q}_S^\theta = 0$ yields

$$2c\Big(\frac{\alpha^2+\beta^2}{\alpha} - \frac{kd_\theta}{2c}\Big)\frac{\beta^2-\alpha^2}{\alpha^2} \;=\; 2c_1 k a_\theta \tag{4.7}$$

$$2c\Big(\frac{\alpha^2+\beta^2}{\alpha} - \frac{kd_\theta}{2c}\Big)\frac{\beta}{\alpha} \;=\; c_1 k b_\theta. \tag{4.8}$$

We first examine the cases $\theta = 0$ and $\theta = \pi/2$. In these cases, $b_\theta = 0$ and $|a_\theta| = 1$, so that from (4.8) we get $\beta = 0$, since $(\alpha^2+\beta^2)/\alpha \neq kd_\theta/(2c)$ in the interior of $\mathcal{V}_S$. Setting $\beta = 0$ in (4.7) we then get $\alpha = -\frac{k}{2c}(c_1 a_\theta + c + c_2)$. Now, an easy calculation shows that in the case $\theta = 0$ the point (α_0^S, β_0^S) lies in the interior of $\mathcal{V}_S$ and it is the global minimiser of $\overline{Q}_S^\theta$. On the other hand, in the case $\theta = \pi/2$ another easy computation shows that the the point $(-kc_2/c, 0)$ lies in $\mathcal{D}_S$ and it is thus not a critical point of our function in the interior of $\mathcal{V}_S$. Then, comparing the values of $\overline{Q}_S^{\pi/2}$ on the boundaries of $\mathcal{D}_S$ and $\mathcal{U}_S$, we find that the minimum is achieved at $(\alpha_{\pi/2}^S, \beta_{\pi/2}^S) = (0,0)$. Moreover, it can be readily checked that (4.6) holds for $\theta = 0$ and $\theta = \pi/2$.

Consider now an arbitrary $\theta \in (0,\pi) \setminus \{\pi/2\}$ and note that in this case $b_\theta \neq 0$ and $|a_\theta| < 1$. As before, we search for critical points of $\overline{Q}_S^\theta$ in the interior of $\mathcal{V}_S$. From (4.8) we get in particular $\beta \neq 0$. Therefore, we may divide (4.7) by (4.8) getting

$$\frac{\beta^2-\alpha^2}{\alpha} = 2\frac{a_\theta}{b_\theta}\beta, \tag{4.9}$$

and in turn that $|\alpha| = |a_\theta \alpha - b_\theta \beta|$. Hence, either $\alpha = a_\theta\alpha - b_\theta\beta$ or $\alpha = b_\theta\beta - a_\theta\alpha$. Suppose that the former case holds true or, equivalently, that

$$\frac{\beta}{\alpha} = \frac{a_\theta - 1}{b_\theta}. \tag{4.10}$$

Before proceeding, consider the second expression for $\overline{Q}_S^\theta$ in $\mathcal{V}_S$ given in Remark 4.1, namely

$$\overline{Q}_S^\theta \;= c\Big(\frac{\beta^2-\alpha^2}{\alpha} - \frac{kd_\theta}{2c}\Big) + \overline{Q}_{S,2}^\theta(\alpha,\beta).$$

Differentiating it with respect to β and setting $\partial_\beta \overline{Q}_S^\theta = 0$ yields

$$2c\Big(\frac{\beta^2-\alpha^2}{\alpha} - \frac{kd_\theta}{2c}\Big)\frac{\beta}{\alpha} = c_1 k b_\theta - 4c\beta.$$

This expression, coupled with (4.9) and (4.10), easily gives

$$(\alpha,\beta) = \frac{k}{2}\left(\frac{b^2}{a_\theta - 1}, b_\theta\right).$$

Recalling the definition of a_θ and b_θ, this point coincides with $(\alpha_\theta^S, \beta_\theta^S)$ defined in the statement, and lies in the interior of $\mathcal{V}_S$. Supposing now that $\alpha = b_\theta\beta - a_\theta\alpha$ and proceeding in a similar manner returns the point

$$-\frac{kc_2}{2c}\left(\frac{b_\theta^2}{a_\theta+1}, b_\theta\right)$$

which belongs to $\mathcal{D}_S$. Hence, the only critical point in the interior of $\mathcal{V}_S$ is $(\alpha_\theta^S, \beta_\theta^S)$. Other computations show that this is indeed the global minimiser of $\overline{Q}_S^\theta$ and that (4.6) holds true. □

Remark 4.2 (Spontaneously curved LCE splay-bend ribbons). In view of the above lemma, we have that the minimum of our limiting functional (4.1) is

$$\min_{\mathcal{A}} \mathscr{J}_S^\theta \;=\; \ell \min_{\mathbb{R}^{2\times 2}} \overline{Q}_S^\theta \;=\; \ell\, \bar{e}_S \;=\; \mu\, \ell\, (1+\lambda) \left(\frac{\pi^4-12}{32}\right) \frac{\eta_0^2}{h_0^2},$$

where in the second equality we have used (4.6) and in the last one the constant $\bar{e}_S$ has been replaced by its expression given in terms of the 3D parameters (the first expression in (2.3)). Also, the minimisers of $\mathscr{J}_T^\theta$ are all the triples $(d_1, d_2, d_3) \in \mathcal{A}$ such that

$$\begin{aligned}(d_1' \cdot d_3\,,\, d_2' \cdot d_3) \;&=\; \frac{k}{2}\Big(-1-\cos 2\theta, \sin 2\theta\Big) \\ &=\; \frac{3\,\eta_0}{\pi^2 h_0}\Big(-1-\cos 2\theta, \sin 2\theta\Big), \qquad\qquad \theta \in [0,\pi),\end{aligned}$$

where in the second expression we have used (2.2). For the convenience of the reader, we list some cases explicitly:

$$\begin{aligned}
&\theta = 0: && (d_1' \cdot d_3, d_2' \cdot d_3) \;=\; \frac{3\,\eta_0}{\pi^2\, h_0}(-2,0);\\
&\theta = \pi/8: && (d_1' \cdot d_3, d_2' \cdot d_3) \;=\; \frac{3\,\eta_0}{\pi^2\, h_0}\left(-\frac{\sqrt{2}+2}{2}, \frac{\sqrt{2}}{2}\right);\\
&\theta = \pi/4: && (d_1' \cdot d_3, d_2' \cdot d_3) \;=\; \frac{3\,\eta_0}{\pi^2\, h_0}(-1,1);\\
&\theta = \pi/2: && (d_1' \cdot d_3, d_2' \cdot d_3) \;=\; (0,0).
\end{aligned}$$

The (minimal energy) configurations of the corresponding rods can be computed and plotted as described in Remark 3.1. Except for the case $\theta = \pi/2$, they are all spiral ribbons, with flexure and torsion given by explicit formulas.

Remark 4.3. Generically, by Taylor-expanding at order two around a minimum the energy densities we have derived, one obtains a 1D free-energy functional of the form

$$\mathscr{J} \;=\; \int_{-\ell/2}^{-\ell/2} C_1(\alpha-\alpha_0)^2 + C_2(\beta-\beta_0)^2 + C_3\alpha\beta + C_4, \tag{4.11}$$

where α and β stand here for the flexure and torsion functions $d_1' \cdot d_3$ and $d_2' \cdot d_3$, respectively. For example, for $\theta = 0$ in the splay-bend case, we have $\alpha_0 = -k$, $\beta_0 = 0$, $C_1 = c$, $C_2 = 2c_1$, $C_3 = 0$, and $C_4 = \bar{e}_S$. By contrast in some cases (e.g. for $\theta = \pi/2$), the Hessian at the minimiser is not positive definite and the quadratic approximation (4.11) fails.

The 1D energies obtained in Section 2 and, in particular, those obtained for twist and splay-bend LCE ribbons in Sections 3 and 4 are, however, far from being quadratic. The difference between such energies and (4.11) is, in most cases, quite dramatic and it becomes apparent far away from the minima. This may lead to the fact that interesting behaviour in the presence of externally applied loads is missed if, instead of using the 1D functionals we have derived, one replaces them with those obtained by a quadratic approximations of the integrands, such as in (4.11).

Acknowledgements. We gratefully acknowledge the support by the European Research Council through the ERC Advanced Grant 340685-MicroMotility. This work was started after an inspiring lecture given by Prof. R. Paroni at "Physics and Mathematics of Materials: current insights", an international conference in honour of the 75th birthday of Paolo Podio-Guidugli held at Gran Sasso Science Istitute (L'Aquila) in January 2016.

The authors declare that they have no conflict of interest.

References

[1] E. Acerbi, G. Buttazzo, and D. Percivale. A variational definition of the strain energy for an elastic string. *Journal of Elasticity*, 25(2): 137–148, 1991.

[2] V. Agostiniani, T. Blass, and K. Koumatos. From nonlinear to linearized elasticity via Γ-convergence: the case of multiwell energies satisfying weak coercivity conditions. *Math. Models Methods in Appl. Sci.*, 25(01):1–38, 2015.

[3] V. Agostiniani, G. Dal Maso, and A. DeSimone. Attainment results for nematic elastomers. *Proc. Roy. Soc. Edinburgh Sect. A*, 145:669–701, 8 2015.

[4] V. Agostiniani and A. DeSimone. Rigorous derivation of active plate models for thin sheets of nematic elastomers. http://arxiv.org/abs/1509.07003.

[5] V. Agostiniani and A. DeSimone. Ogden-type energies for nematic elastomers. *Internat. J. Non-Linear Mech.*, 47(2):402–412, 2012.

[6] H. Aharoni, Y. Abraham, R. Elbaum, E. Sharon, and R. Kupferman. Emergence of spontaneous twist and curvature in non-euclidean rods: application to *Erodium* plant cells. *Phys. Rev. Lett.*, 108:238106, Jun 2012.

[7] H. Aharoni, E. Sharon, and R. Kupferman. Geometry of thin nematic elastomer sheets. *Phys. Rev. Lett.*, 113:257801, Dec 2014.

[8] M. Arroyo and A. DeSimone. Shape control of active surfaces inspired by the movement of euglenids. *J. Mech. Phys. Solids*, 62:99 – 112, 2014. Sixtieth anniversary issue in honor of Professor Rodney Hill.

[9] M. Arroyo, L. Heltai, D Millán, and A DeSimone. Reverse engineering the euglenoid movement. *PNAS*, 109(44):17874 – 17879, 2012.

[10] P. Bladon, E. M. Terentjev, and M. Warner. Transitions and instabilities in liquid crystal elastomers. *Phys. Rev. E*, 47:R3838–R3840, Jun 1993.

[11] S. Conti, A. DeSimone, and G. Dolzmann. Semisoft elasticity and director reorientation in stretched sheets of nematic elastomers. *Phys. Rev. E*, 66:061710, Dec 2002.

[12] S. Conti, A. DeSimone, and G. Dolzmann. Soft elastic response of stretched sheets of nematic elastomers: a numerical study. *J. Mech. Phys. Solids*, 50(7):1431 – 1451, 2002.

[13] C Dawson, J. F. V. Vincent, and A.-M. Rocca. How pine cones open. *Nature*, 290:668, 1997.

[14] A. DeSimone. Energetics of fine domain structures. *Ferroelectrics*, 222:275–284, 1999.

[15] A. DeSimone and G. Dolzmann. Macroscopic response of nematic elastomers via relaxation of a class of SO(3)-invariant energies. *Arch. Ration. Mech. Anal.*, 161(3):181–204, 2002.

[16] A. DeSimone and L. Teresi. Elastic energies for nematic elastomers. *Eur. Phys. J. E*, 29:191–204, 2009.

[17] E. Efrati. Non-Euclidean ribbons. *J. Elasticity*, 119(1):251–261, 2014.

[18] P. Fratzl and F. G. Barth. Biomaterial systems for mechanosensing and actuation. *Nature*, 462:442–448, 2009.

[19] L. Freddi, P. Hornung, M. G. Mora, and R. Paroni. A corrected Sadowsky functional for inextensible elastic ribbons. *J. Elasticity*, pages 1–12, 2015.

[20] G. Friesecke, R. D. James, and S. Müller. A theorem on geometric rigidity and the derivation of nonlinear plate theory from three-dimensional elasticity. *Comm. Pure Appl. Math.*, 55(11):1461–1506, 2002.

[21] M. H. Godinho, J. P. Canejo, G. Feio, and E. M. Terentjev. Self-winding of helices in plant tendrils and cellulose liquid crystal fibers. *Soft Matter*, 6:5965–5970, 2010.

[22] J. Kim, J. A. Hanna, M. Byun, C. D. Santangelo, and R. C. Hayward. Designing responsive buckled surfaces by halftone gel lithography. *Science*, 335(6073):1201–1205, 2012.

[23] N. O. Kirby and E. Fried. Gamma-limit of a model for the elastic energy of an inextensible ribbon. *J. Elasticity*, 119(1):35–47, 2014.

[24] Y. Klein, E Efrati, and E Sharon. Shaping of elastic sheets by prescription of non-euclidean metrics. *Science*, 315(5815):1116–1120, 2007.

[25] M. Lewicka and R. Pakzad. Scaling laws for non-Euclidean plates and the $W^{2,2}$ isometric immersions of Riemannian metrics. *ESAIM: Control Optim. Calc. Var*, 17(4):1158–1173, 11 2011.

[26] E. Reyssat and L. Mahadevan. Hygromorphs: from pine cones to biomimetic bilayers. *Journal of The Royal Society Interface*, pages 951—957, 2009.

[27] Y. Sawa, K. Urayama, T. Takigawa, A. DeSimone, and L. Teresi. Thermally driven giant bending of liquid crystal elastomer films with hybrid alignment. *Macromolecules*, 43:4362–4369, May 2010.

[28] Y. Sawa, F. Ye, K. Urayama, T. Takigawa, V. Gimenez-Pinto, R. L. B. Selinger, and J. V. Selinger. Shape selection of twist-nematic-elastomer ribbons. *PNAS*, 108(16):6364–6368, 2011.

[29] B. Schmidt. Plate theory for stressed heterogeneous multilayers of finite bending energy. *J. Math. Pures Appl.*, 88(1):107 – 122, 2007.
[30] A. Shahaf, E. Efrati, R. Kupferman, and E. Sharon. Geometry and mechanics in the opening of chiral seed pods. *Science*, 333(6050):1726–1730, 2011.
[31] A. R. Studart and R. M. Erb. Bioinspired materials that self-shape through programmed microstructures. *Soft Matter*, 10:1284–1294, 2014.
[32] L. Teresi and V. Varano. Modeling helicoid to spiral-ribbon transitions of twist-nematic elastomers. *Soft Matter*, 9:3081–3088, 2013.
[33] A. C. Trindade, J. P. Canejo, P. I. C. Teixeira, P. Patricio, and M. H. Godinho. First curl, then wrinkle. *Macromolecular Rapid Communications*, 34(20):1618–1622, 2013.
[34] K. Urayama. Switching shapes of nematic elastomers with various director configurations. *Reactive and Functional Polymers*, 73(7):885–890, 2013. Challenges and Emerging Technologies in the Polymer Gels.
[35] M. Warner and E. M. Terentjev. *Liquid crystal elastomers*. Clarendon Press, Oxford, 2003.

SISSA, via Bonomea 265, 34136 Trieste - Italy
E-mail address: vagostin@sissa.it

SISSA, via Bonomea 265, 34136 Trieste - Italy
E-mail address: desimone@sissa.it

Gran Sasso Science Institute, viale Francesco Crispi 7, 67100 L'Aquila - Italy
E-mail address: konstantinos.koumatos@gssi.infn.it